Journal of Radiation Research, 2012, 53, 989–998
doi: 10.1093/jrr/rrs050 Advance Access Publication 21 August 2012

Regular Paper

Evaluation of effective dose for a patient under Ga-67 nuclear examination using TLD, water phantom and a simplified model

Kuang Hua CHU[1,2], Yu Ting LIN[1,3], Chia Chun HSU[1,4], Chien Yi CHEN[5] and Lung Kwang PAN[1,*]

[1]Graduate Institute of Radiological Science, Central Taiwan University of Science and Technology, Takun, Taichung 40609, Taiwan
[2]Cardiovascular Center, Taichung Veterans General Hospital, Taichung 40705, Taiwan
[3]Department of Radiology, China Medical University Beigang Hospital, Yunlin 65152, Taiwan
[4]Department of Radiology, Buddhist Tzu Chi General Hospital, Taichung Branch, Taichung County 427, Taiwan
[5]School of Medical Imaging and Radiological Science, Chung Shan Medical University, Taichung 402, Taiwan
*Corresponding author. Graduate Institute of Radiological Science, Central Taiwan, University of Science and Technology, Takun, Taichung 406, Taiwan. Tel: 886-4-2239-1647 ext. 7109; Fax: 886-4-2239-6762; Email: lkpan@ctust.edu.tw

(Received 10 April 2012; revised 8 June 2012; accepted 12 June 2012)

This study evaluated the effective dose of Ga-67 for a patient undergoing Ga-67 citrate nuclear examination by applying thermoluminescent dosimeter (TLD) technique and an indigenous water phantom. The Ga-67 radionuclide remaining in the body inevitably generated a measurable internal dose even though gamma camera scanning took only minutes to complete the clinical examination. For effective simulation of the cumulated effective dose for a patient undergoing examination, 150 TLDs were placed inside the water phantom for 6 days to monitor the gamma ray dose from the distributed Ga-67 citrate solution. The inserted TLDs represented internal organs, and the effective dose was calculated according to data in the ICRP-60 report. The water phantom was designed to model the body of a healthy human weighing 70 kg, and the water that was mixed with Ga-67 citrate solution was slowly replaced with fresh feed water to yield the required biological half life of the phantom. After continuously feeding in fresh water throughout the 6 days of TLD exposure, the TLDs were analyzed to determine the effective doses from the various biological half lives of the phantom. The derived effective dose of 185 MBq Ga-67 citrate solution for male/female (M/F) was 10.7/12.2, 10.7/12.0, 8.7/9.9 and 6.0/6.8 mSv, of biological half lives of 6.0, 4.5, 3.0 and 1.5 days, respectively. Although these experimental results correlated well with earlier empirical studies, they were lower than most calculated values. The cumulated uncertainty in the effective dose was 12.5–19.4%, which was acceptable in terms of both TLD counting statistic and reproducibility.

Keywords: water phantom; internal dose; TLD, transient equilibrium; dose verification

INTRODUCTION

To evaluate the effective dose of Ga-67 for a patient undergoing Ga-67 citrate nuclear examination, this study used an indigenous water phantom, the thermoluminescent dosimeter (TLD) technique and a simplified model. Unlike X-ray diagnosis, in which the patient is passively and only momentarily exposed to low-dose X-rays, gamma camera scintigraphy exposes the patient to a high internal dose. Patients who undergo nuclear examination are initially injected with a compound solution containing a specific radionuclide before being scanned with a gamma camera to obtain scintigraphy images for clinical diagnosis.

Although nuclear examination requires only minutes for data acquisition, excretion of the radioactive solution may take days. Until it is eventually excreted by metabolic mechanisms, the radioactive solution remains in the bodies of patients after they undergo Ga-67 nuclear examination. Studies of this topic in recent decades have developed many theoretical simulations of the cumulative dose of radioactive nuclides since each nuclide has a unique radioactive fingerprint. Although most theoretical studies of this issue have applied the medical internal radiation dose (MIRD) calculation model, their conclusions are highly variable [1–10]. Practical studies of internal dose are rarely performed and their results are even more inconsistent

[11–15]. The disagreements among both theoretical and practical investigations may result from incorrect research assumptions or oversimplifications.

The many radionuclides used for clinical diagnosis include the radiopharmaceutical ^{67}Ga-citrate, which was originally developed for bone scintigraphy before later being applied in diagnosing malignant lymphomas, hepatic tumors and melanomas [16]. Patients who undergo routine nuclear examinations must wait 3 or 4 hours after receiving an initial injection of 185 MBq Ga-67 citrate solution so that the radio-labeled solution can adequately disperse in the body and enable data collection. Therefore, this study effectively simulated this unique situation by using an indigenous water phantom for precise modeling of the Ga-67 nuclear examination process. After sealing and placing several hundred well-calibrated TLD-100s in the phantom for several days to obtain the cumulative gamma ray dose in the represented organ locations, the ICRP-60 report is used to calculate the effective dose. The TLD is calibrated by either practical measurement or by theoretical computation in a preliminary study, since TLD in water must be specifically considered. A simple model based on the transient equilibrium in the radionuclide chain decay theorem is used to calculate the effective dose. The model assumes that the biological-half-life of the Ga-67 citrate solution determines the internal dose accumulation. That is, the model calculates the effective doses based on the biological half-lives of the Ga-67 radionuclide.

EFFECTIVE DOSE

The ICRP committees have been quantifying personal radiation doses for many decades. In 1990, ICRP-60 [17] defined effective dose, E, as the quantity surveyed by personal dosimetry, which is calculated as

$$E = \sum_T \omega_T \times H_T \quad (1)$$

Where ω_T is a tissue or organ weighting factor and H_T is the tissue or organ equivalent dose, which is given by:

$$H_T = \sum_\gamma \omega_\gamma \times D_{T,\gamma} \quad (2)$$

Where ω_r is the weighting factor of the incident radiation and $D_{T,\ r}$ is the mean dose of incident radiation of type γ absorbed by the organ or tissue T; that is, the effective dose can be determined directly by multiplying the equivalent dose for each organ or tissue by the corresponding weighting factors [Eq. 2].

In ICRP-26, ω_T values were specifically assigned to only six organs. For analytical purposes, the five organs that received the next highest dose equivalents were combined into a pseudo-organ called the 'remainder' [18]. In ICRP-60, the number of organs that were assigned ω_T values was much larger, and previous values of ω_T were updated as the understanding of cancer risk from exposure of these organs to radiation improved. The pseudo-organ, 'remainder', was also re-defined in ICRP-60 and defined as ten specific organs. Since the ω_T values of the various organs were independent of H_T delivery, the ICRP-26 definition of H_E can be extended to include updated values of ICRP-60 ω_T, which increases accuracy when estimating E.

EXPERIMENT

This work evaluated the effective dose, E, of Ga-67 citrate in a Ga-67 citrate nuclear examination of an adult patient of either gender. Each organ or tissue of interest was assigned a ω_T value based on three to five TLD-100s. The counts were then used to calculate the effective dose based on the equivalent dose for each organ or tissue (Eqs 1–2).

Water phantom

Figure 1 shows the graph (**A**) and the actual water phantom (**B**) used herein. The computerized plot shows the fine structure in a precise scale of the water phantom. The phantom, which was designed to model a 70-kg human body (including thoracic, abdominal and pelvic cavities) consisted of an elliptical acrylic (polymethylmethacrylate, PMMA) box (700 mm high, with a major elliptical axis of 200 and a minor axis of 100 mm) containing 44.0 kg of water (mass = $20 \times 10 \times 70 \times \pi$ [cm^3] $\times 0.001$ [kg/cm^3] = 44.0 [kg]). Figure 1 clearly shows that the feed water tube was inserted through the tube in the center of the top of the

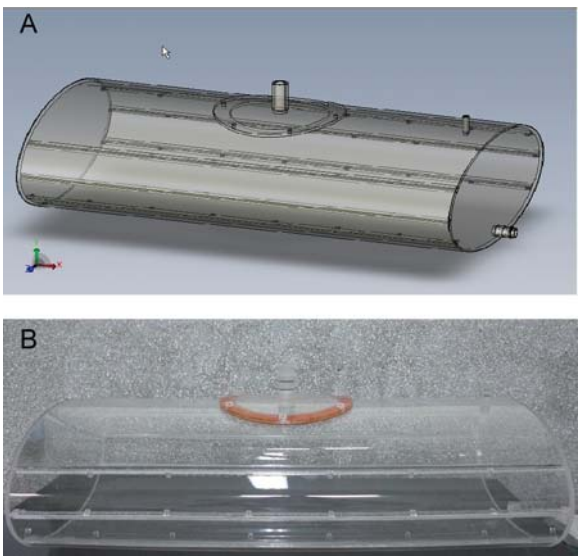

Fig. 1. (**A**) The computerized plot of the water phantom, (**B**) the water phantom that was used herein. The phantom was an elliptical acrylic (polymethylmethacrylate, PMMA) box (700 mm high, with a major elliptical axis of 200 and a minor axis of 100 mm).

box. The overflow then flows from the drain tube on the top-tail of the box. The feed water can be adjusted to model various human metabolic mechanisms. For example, continuously filling the box with feed water at 5 cm^3/min was equivalent to replacing half of the water phantom in 3.05 days (22,000 [cm^3] / (5 [cm^3/min.] ×60 [min/h] ×24 [h/day]) = 3.05 [day]). The feed water input must be precisely controlled because the residence time of radioactive Ga-67 citrate solution in the phantom determined the internal dose. Therefore, the feed water input to the phantom was precisely controlled with an automatic infusion device used for clinical intravenous infusion.

An actual gamma camera scan of a male body (76 kg, 172 cm, BMI = 25.7) was inspected to determine whether the indigenous water phantom could effectively simulate the human body undergoing nuclear examination. The image was obtained by a 10 min scan of a male patient performed 4 h after the patient had been injected with 148 MBq of Ga-67 citrate solution. Figure 2 clearly shows that the counts/pixels in the (0) stomach, (1) lumbar-spine, (2) liver and (3) whole body (regions of interest, ROI, 0, 1, 2 and 3) were (0) 10.2 (3661/360 = 10.2), (1) 16.6 (5960/360 = 16.6), (2) 21.5 (7734/360 = 21.5) and (3) 11.4 (580 733/50 720 = 11.4), respectively. The indigenous water phantom defined the body in terms of thoracic, abdominal and pelvic cavities. The variation in count/pixel values was negligible throughout the body even though the count/pixel was higher in a few critical organs than in other regions. However, the simplified model confirmed that the human body could still be represented as a homogenous body of water in which Ga-67 citrate solution was well distributed since large variations in the acquired count/pixel were limited to only a few regions and to a comparatively short time during the actual gamma camera scan.

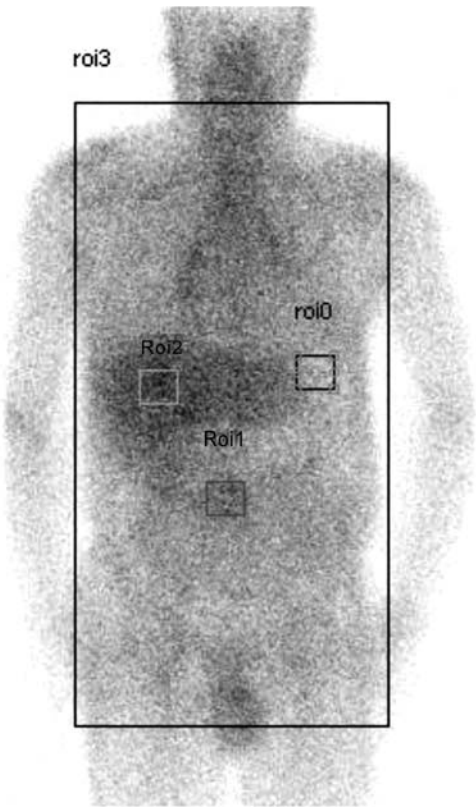

Fig. 2. Routine gamma camera scanning. A male patient was administered Ga-67 citrate solution with a radioactivity of 148 MBq and examined for 10 min after a 4-h waiting time. The ROIs 0, 1, 2 and 3 were the (0) stomach, (1) lumbar-spine, (2) liver and (3) whole body, respectively.

Preliminary survey of biological half life

A preliminary survey was performed to evaluate the biological half-life of the Ga-67 radionuclide in six patients (2M/4F, ages 25–50 years). The Ga-67 citrate nuclear examination in each patient was performed by rapid screening with a gamma camera (SIEMENS E. CAM) at Chung Shan Medical University Hospital (CSMUH). The ROI in each patient was the neck to the thigh, and the counting protocol was a 10-min scan performed 30 min after injection with the Ga-67 citrate solution followed by 30-min scans every 12 h for 3 days. Therefore, six sets of counts/pixel data were obtained as a function of elapsed time. The biological half-life, T_B, of the Ga-67 radionuclide in the whole body of each patient could thus be determined. The average T_B derived for the whole body (defined as ROI 3 in Fig. 2) was 1.86 ± 0.45 days (max T_B: 2.63 days, min T_B: 1.38 days). Additionally, Arsos *et al.* reported a 4.9-day biological half-life for intravenously injected Ga-67 citrate solution [19]. Another study of human metabolic mechanisms by Priest *et al.* reported a 4.7-day biological half life [20]. Thus, T_B was adjusted to 1.5, 3.0, 4.5 and 6.0 days, respectively, to obtain the practical effective dose in this work.

TLD calibration

Calibration was performed by placing 150 TLD-100s (LiF: Mg, Ti) (3 × 3 × 0.9 mm^3, Harshaw) in the center of a spherical water tank (diameter, 40 cm) for 24 h and then recording radioactive emissions from the TLD readout system. The absorbed dose D_r of the TLD at that position after a fixed period, t, was calculated by a simplified Eq. 3 [21] or by a theoretical simulation performed using MCNP code [22].

$$D_\gamma(t) = \sum_{i=1}^{n} \phi_i \times E_i \times I_r \times \left(\frac{\mu}{\rho}\right)_{abi} \times \frac{1 - e^{-\mu_i r}}{\mu_i} \times \frac{1 - e^{-\lambda t}}{\lambda} \quad (3)$$

Where Φ is the beam flux and E is the gamma ray energy of the Ga-67 radionuclide. The I_i is the branching ratio of

Table 1. The precise data concerning the Ga-67 radionuclide that are used to calculate the absorbed dose in this work

E (MeV)	I_i (%)	$(\mu/\rho)_i$ (cm^2/g)	μ_i (cm^{-1})	Center dose (Gy/s)
0.091	3.07	0.0259	0.1895	4.00E-10
0.093	37.80	0.0258	0.1878	5.02E-09
0.185	20.90	0.0291	0.1416	6.01E-09
0.209	2.37	0.0299	0.1347	7.87E-10
0.300	16.80	0.0319	0.1161	8.41E-09
0.394	4.66	0.0327	0.1039	3.11E-09
0.484	0.07	0.0330	0.0954	5.66E-11
0.703	0.01	0.0325	0.0819	1.32E-11
0.794	0.05	0.0321	0.0779	6.92E-11
0.888	0.15	0.0316	0.0744	2.16E-10
Sum				**2.41E-08**
MCNP simulation				**3.10E-08**

the specific gamma ray energy. The $(\mu/\rho)_{abi}$ and μ_i are the real mass absorption coefficient and linear attenuation coefficient of water, respectively, at a particular gamma ray energy. The decay constant λ is defined as the reciprocal of only the physical half-life of the Ga-67 radionuclide because the biological half-life of this radionuclide is zero under these conditions. Table 1 presents the actual Ga-67 radionuclide data used to calculate the absorbed dose. Table 1 clearly shows that the outcome based on the MCNP estimate, 3.10E-8 Gy/s, exceeds that based on the simplified equation, 2.41E-8 Gy/s, since the equation does not consider auger electrons, delta rays or Compton electron scattering mechanisms. However, the simplified equation still provides useful data for determining the lowest absorbed dose.

Data collection

The water phantom was divided into equal sections separated by three horizontal planes (coronal cross sections). On all planes, acrylic hooks installed on both sides of the inner wall of the phantom at 10-cm intervals across each plane were tied together with plastic string to form a web system for holding the TLDs (Fig. 1). Figure 3 presents the precise positions of the TLDs in each coronal cross section. Three to five TLDs were separately sealed inside two layers of waterproof polyethylene (PE) bags before being placed inside the phantom to monitor radioactivity in internal organs or tissues.

After loading the TLDs, the phantom was filled with 44.0 kg fresh water. A Ga-67 citrate solution with a radioactivity of 74 MBq was then added through the tube at the

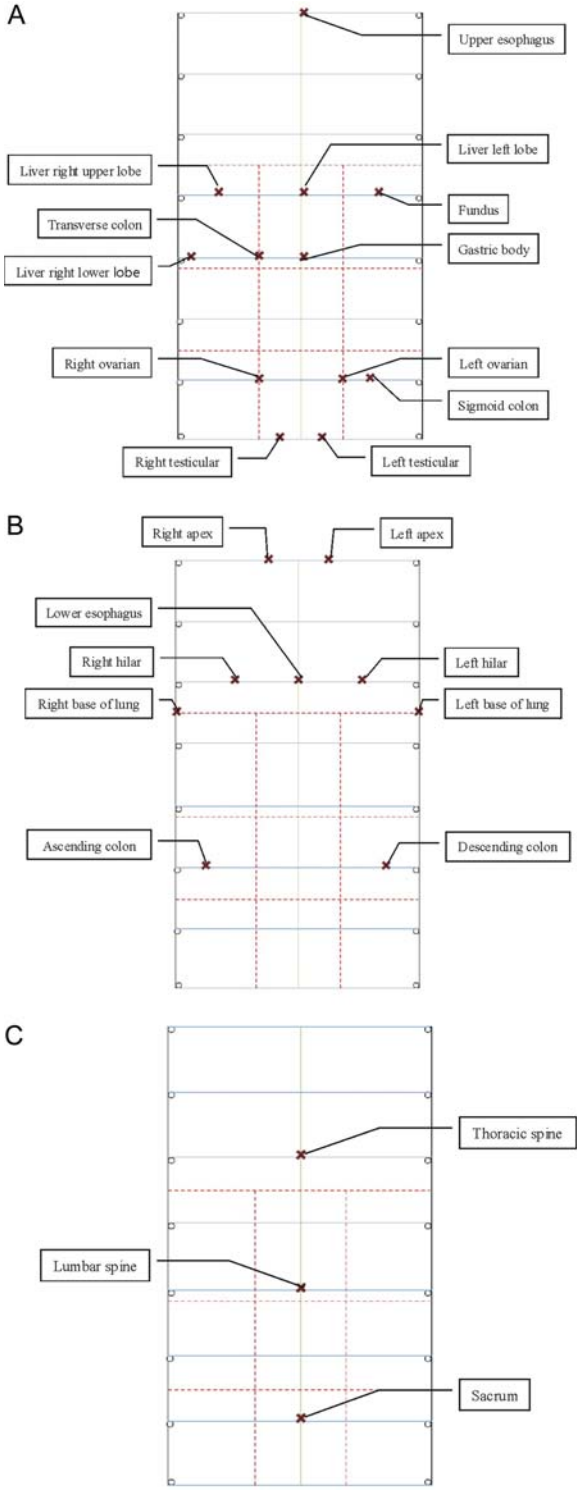

Fig. 3. The precise positions of the TLDs in each coronal cross section (**A**) upper, (**B**) medium and (**C**) bottom. Three to five TLDs were separately sealed inside PE bags, which were placed in another water-proof PE bag inside yet another water-proof bag before being placed inside the phantom to monitor the radioactivity of the internal organ or tissue.

center of the top of the phantom (Fig. 1). After letting the Ga-67 citrate sit for 1 h to ensure a uniform distribution, fresh water was fed through the tube to replace the water mixed with the Ga-67 radionuclide in the preceding stage. Precise control of the amount of feed water injected by the automatic infusion device, which enabled adjustment of the half replacement time of the radioactive water inside the phantom to 1.5, 3.0, 4.5 and 6.0 days. The half replacement time of the radioactive water was effectively the biological half-life of the Ga-67 radionuclide in a standard -g male body. Increasing the half replacement time of the radioactive water increased the concentration of Ga-67 radioactive solution maintained inside the phantom and increased the resulting internal dose.

TLD readout

The exposed TLDs were measured and analyzed with a TLD reader (RA94, MIKROLAB) before annealing in a Barnstead International model 19200 at 400°C for 1 h followed by further annealing in a Barnstead International model 47900 at 100°C for 2 h. The reading of each exposed TLD was not recorded until 28 h later to ensure a stable TLD glow curve. The TLD counts were recorded by a read out system with a 2-s holding time and heated at a rate of 5°C/s to enable data acquisition over a temperature range of 50–180°C. The TLD readout system was optimized using the Taguchi method [23].

DATA ANALYSIS AND RESULTS

Error compiling

Table 2 shows the error for each derived effective dose, E, for various biological half-lives, which was calculated as the square root of the sum of the squares of the individual errors, Δ_i. The uncertainty in ω_T was defined as 5% because the weighting factor was normalized. The internal normalization errors for TLDs were obtained from the preliminary survey of all TLDs. Since the phantom consisted of only pure water, the uncertainty associated with non-tissue equivalence effects of the water phantom was defined to a maximal 10%. The specific value of uncertainty was estimated from the weighted average of the various organ volumes [24, 25].

Table 2. The systematic and random errors for the practical evaluation of effective dose, E, in this investigation

Source	One standard deviation Δ_i
Others:	
ω_T (tissue or organ weighting factor)	5%
TLD calibration	2–6%
TLD internal normalization	1.1–7.4%
non-tissue equivalence effects	10%
feed water infusion rate	5%
Measurement:	
TLD counting statistics	0.4–11.6%
Δ_{tot}	12.5–19.4%

Because the non-tissue equivalence effects are related to variation in Compton scattering electrons used to determine doses for the soft tissue, rib or spine in the phantom, they may result in inaccurate estimates of the scattering effect. This effect can be estimated by a Monte-Carlo simulation of a digital homogeneous or heterogeneous phantom exposed to a similar gamma ray field. The total error was dominated by the statistical error in counting, which could be suppressed by repeated measurements. Averaging the data from three independent trials obtained a maximum counting statistical error and total error of 11.6% and 19.4%, respectively.

Effective dose

Table 3 presents the effective dose, E, which was determined according to the various set biological half-lives of the 74-MBq Ga-67 citrate solution used in the nuclear examination. The tissue weighting factors, ω_T, for the various internal organs or tissues are also presented. The effective dose, E, was determined by multiplying ω_T by the corresponding equivalent dose, H_T, which was itself obtained by multiplying each TLD count by the relevant calibration factor. The use of similar exposure conditions based on preliminary measurements simplified the conversion of TLD counts into specific equivalent doses for each organ of interest.

DISCUSSION

Comparisons with E values obtained elsewhere

Table 3 shows that the effective dose, E, was derived using a 6-day counting period and then extended to infinite time by multiplying it by the correction factor (CF) obtained by Eq. 4.

$$CF = \frac{1-e^{-\lambda t_\infty}}{\lambda} \Big/ \frac{1-e^{-\lambda t_c}}{\lambda} = \frac{1}{\lambda} \Big/ \frac{1-e^{-\lambda t_c}}{\lambda} = 1/(1-e^{-\lambda t_c}) \quad (4)$$

Where t_c is the counting period, which was 6 days, in this investigation, and λ is the decay constant for each of the effective half lives, T_E. CFs were 1.02, 1.07, 1.12 and 1.16 for T_E values of Ga-67 of 1.03, 1.56, 1.89 and 2.11 days, respectively. The corresponding T_B of the water phantom was adjusted to 1.5, 3, 4.5 and 6 days based on the decay constant λ obtained by Eq. 4. Apparently, the short T_B of the

Table 3. The effective dose, *E*, which is determined using the various biological half life settings of the 74-MBq Ga-67 citrate solution used in nuclear examination

Organ or tissue (mSv)	Biological half-life (day)					
	ICRP-60 ω_T	ICRP-103 ω_T	1.5	3	4.5	6
Gonad (testicular)	0.2	0.08	1.54	1.94	2.05	2.28
Gonad (ovarian)	0.2	0.08	3.16	3.97	4.17	4.69
Red bone marrow	0.12	0.12	3.53	4.71	5.29	5.40
Colon	0.12	0.12	3.14	4.19	5.04	4.68
Lung	0.12	0.12	2.46	3.17	3.85	3.57
Stomach	0.12	0.12	3.00	4.65	5.64	4.48
Bladder	0.05	0.04	0.70	1.90	2.18	2.94
Breast	0.05	0.12	1.19	2.45	2.69	2.73
Liver	0.05	0.04	2.79	3.35	4.27	4.52
Esophagus	0.05	0.04	2.40	3.01	4.29	3.97
Thyroid	0.05	0.04	1.37	1.79	2.26	2.12
Skin	0.01	0.01	1.88	2.39	1.63	2.81
Bone surface	0.01	0.01	1.74	2.22	1.39	2.68
Brain	N/A	0.01				
Salivary glands	N/A	0.01				
remainders	0.05	0.12				
Effective dose, *E (mSv)*:						
Male (ICRP-60/-103)			**2.34/2.38**	**3.23/3.38**	**3.80/3.98**	**3.69/3.83**
Female (ICRP-60/-103)			**2.68/2.53**	**3.66/3.57**	**4.25/4.18**	**4.20/4.05**

The tissue weighting factors, ω_T, for various internal organs or tissues are also presented according to either ICRP-60 or -103 report.

phantom results from the small correction factor since activity inside the phantom is minimal after 6 days. Therefore, the *CF* values used to obtain the internal doses are negligible.

Table 4 shows how the effective doses calculated using various biological half lives are revised by applying the *CF*s. The table includes effective doses obtained in other studies for comparison. Both Dr Saha [12] and Dr Stabins [13] used the MIRDDOSE code [26] to perform simulations, whereas Shanehsazzadeh *et al.* [14, 27] used the MIRDOSE code and verified the results in rat studies before extrapolating the effective dose to humans. The United Nations Scientific Committee on the Effects of Atomic Radiation (UNSCEAR) [15] estimated the effective dose by reviewing medical case reports throughout the United States and determined the effective dose as a function of the weight of the patient. Patients weighting 70, 55, 33, 18 and 10 kg had effective doses of around 18.5, 23.3, 28.1, 28.5 and 34.4 mSv, respectively, in Ga-67 citrate nuclear examination. The derived effective doses herein are consistent with the results reported by both Saha [12] and Shanehsazzadeh [14] but are lower than those reported by Stabin and those recommended by UNSCEAR. A study by Shanehsazzadeh also reported a low effective dose of 5.26 mSv in a recent study performed using a similar approach [27].

Simplified one group model of human body for evaluating effective dose

Theoretical simulations yield highly controversial estimates of the radioactive effective dose; *E*, even though they all are based on the same MIRDOSE code. In contrast, the practical method applied using the water phantom and TLDs herein yields effective doses with the required confidence. The phantom is designed to model the human body as a homogenous volume of water, despite the presence of Ga-67 citrate solution in various organs. However, this simplified dose evaluation method enables the use of the TLD method to determine the radioactive internal dose required for a patient undergoing nuclear examination.

The simplified model assumes that the residence time of the Ga-67 radionuclides in various organs is directly related to the transient equilibrium phenomenon described by the

Table 4. The effective doses that are calculated using various effective half-lives are revised by applying the CF correction; additionally, effective doses that are taken from other studies are also attached for comparison, and all the reported data are calculated according to the ICRP-60 report

Team	Type	Method	Object	*E* (mSv/185 MBq)
Saha [12]	Ga-67 citrate	MIRDOSE 3	Human	13.0
Stabin *et al.* [13]	Ga-67 citrate	MIRDOSE 3	Human (M/F)	18.5/22.2
Shanehsazzadeh *et al.* [14]	Ga-67 DTPA-ACTH	MIRDOSE 3 & animal base	Extrapolating from rat to human (M/F)	10.1/10.3
Shanehsazzadeh *et al.* [27]	Ga-67 cDTPA-GnRH	animal base	Extrapolating from rat to human	5.26
UNSCEAR [15]	Ga-67 citrate	N/A	Human	18.5–34.4
MIRD [28]	Ga-67 citrate	MIRDOSE 3	Human	13.0
SNM [29]	Ga-67 citrate	MIRDOSE 3	Human	22.2
This work				
	Ga-67 citrate	TLD	Phantom	
		T_E = 1.03 days (M/F)		6.0/6.8
		T_E = 1.56 days (M/F)		8.7/9.9
		T_E = 1.89 days (M/F)		10.7/12.0
		T_E = 2.11 days (M/F)		10.7/12.2

Ga-67 nuclear examination via TLD technique

chain decay theorem. This assumption is also supported by the finding reported by the Society of Nuclear Medicine [29] based on consecutive evaluations of patients that 10–25% of the injected dose is excreted by the kidneys during the first 24 h after injection. The main excretion route then changes to the gastrointestinal tract. By 48 h after injection, about 75% of the injected dose remains in the body and is equally distributed among the liver, bone and bone marrow, and soft tissues. Accordingly, the whole body and a series of internal organs, which are defined according to the bio-kinetic model, can be interpreted as the parent compartment and the series of daughter compartments along the same decay chain. Unlike the secular equilibrium in the parent compartment, which has an extremely long decay half-life; the transient equilibrium exists in the bio-kinetic model when the effective half-life of the parent compartment is ten-fold that of the daughter compartment; the activity of the daughter compartment is maximal at time t_{max}. The subsequent decay associated with the effective half-life of the parent is given by Eq. 5 [30].

$$A_d = \lambda_d N_d = \frac{\lambda_d}{\lambda_d - \lambda_p} \cdot A_p = \frac{\lambda_d}{\lambda_d - \lambda_p} \cdot \lambda_p N_p; \qquad t_{\max} = \frac{\ln \lambda_d - \ln \lambda_p}{\lambda_d - \lambda_p} \tag{5}$$

Where λ_d [ln2/$T_E(d)$] and λ_p [ln2/$T_E(p)$] are the decay constants of the daughter (internal organ) and parent (whole body) compartments, respectively. The effective half-life equals the reciprocal of the sum of the reciprocal of the biological half-life and that of the physical half-life (T_E^{-1} = [$T_B^{-1} + T_R^{-1}$]). Therefore, change in the biological half-life of the whole body (parent) compartment determines overall performance since the physical half-life of Ga-67, T_R, is fixed at 78.2 h.

The MIRD-3 code indicates that most daughter compartments have biological half-lives of 1–10 h. For example, the biological half-lives in the stomach, small intestine and upper large intestine are 0.7, 2.7 and 9.2 h., respectively. Therefore, for the internal organ, t_{max} is 4.4–19.3, 5.4–26.0, 5.6–28.0 and 5.8–29.2 h for Ga-67 biological half-lives of 1.0, 3.0, 4.5 and 6.0 days, respectively [Eq. 5]. Specifically, t_{max} equals either 4.4 or 19.3 h if (i) the biological half life of Ga-67 in the internal organ (daughter) is either 1 or 10 h, respectively, and if (ii) the biological half-life of the whole body (parent) is 1.0 day [$T_E(p)/T_E(d)$= 18.4 or 1.8]. In contrast, the t_{max} increases to 5.8 and 29.2 h if the biological half-life of the whole body (parent) is extended from 1.0 day to 6.0 days, respectively. Restated, stabilization of transient phenomenon in the first 1.5 days (~36 h) is followed by decay of the whole body compartment (parent) even in the worst case of dangling (t_{max}= 29.2 h; the biological half-life in a particular internal organ and the whole body is 10 h and 6 days, respectively [$T_E(p)/T_E(d)$ = 5.9]). The 150 TLDs were left inside the water phantom for 6 days, which is longer than the t_{max} for most

of the cases considered herein. Accordingly, the fluctuation of the gross activity of Ga-67 radionuclides in any specific daughter compartment generates an acceptable uncertainty in the real measurement. Although the simplified hypothesis assumes that a single compartment of a body structure may not apply clinically in an actual human body, the obtained data are highly consistent and reproducible.

Isodose plot inside the water phantom

The water phantom is filled with water mixed with Ga-67 citrate solution to model a 70-kg human body undergoing an actual nuclear examination. After keeping the phantom stationary for 1 h to ensure uniform distribution of the radioactive solution, water is fed into the system. Since the filling tube extends from the center top of the phantom to the bottom of the phantom (Fig. 1), the fresh feed water diffuses slowly toward the drain tube. Diffusion in the water phantom may cause the original radioactive solution to accumulate gradually near the drain tube before it overflows. In an actual human, however, biological excretion through the kidney and bladder represents a unique internal diffusion mechanism.

Figure 4 presents several isodose curves in both the coronal and the sagittal directions. The dose is highest near the tail of the middle coronal and near the central sagittal images. Most of the high doses are near the center of the bottom of the phantom since the diffusion mechanism determines the distribution of the dose therein.

TLD glow curve of Ga-67

A glowing curve was plotted according to the recorded TLD counts and responded uniquely to temperature from the TLD readout device. The TLD is sealed in two waterproof PE bags before being placed in the water phantom. Therefore, the TLD is exposed to the radioactivity of the ambient Ga-67 citrate solution. Since the water solvent either moderates or attenuates the incoming gamma rays under these conditions, the original glow curve of the TLD exposed only to the radioactivity of Ga-67 in the air is deformed. Figure 5 plots three glow curves of a single TLD

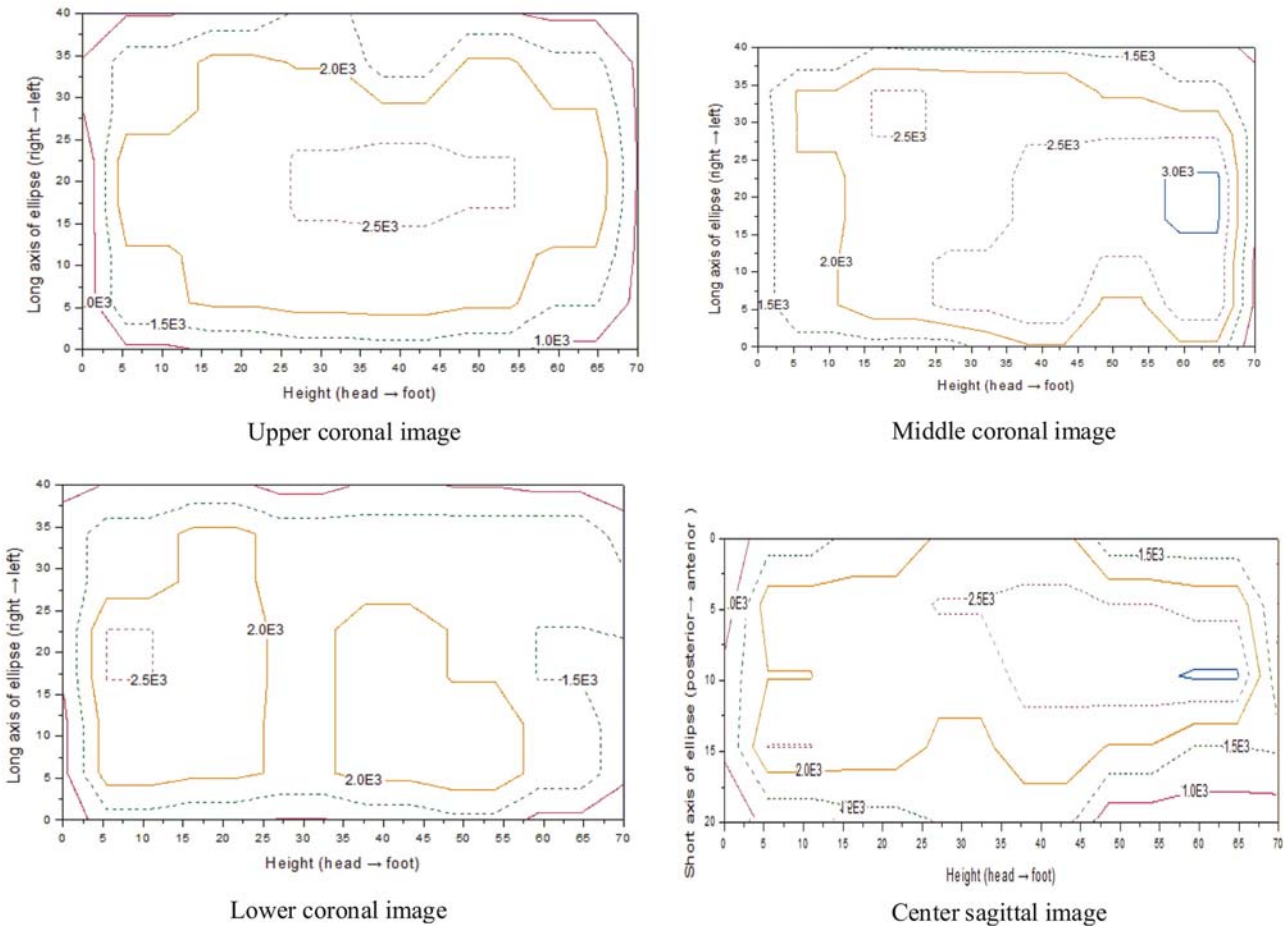

Fig. 4. Four isodose curves from both the coronal and the sagittal directions. The dose is highest close to both the tail of the middle coronal and the central sagittal images. Most of the high doses are close to the center of the bottom of the phantom, because the diffusion mechanism dominates the distribution of the dose therein.

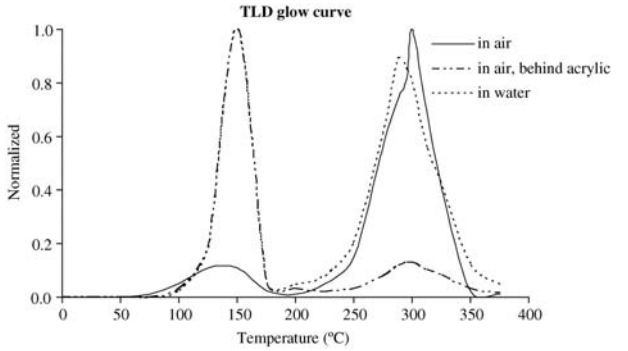

Fig. 5. Three glow curves of a single TLD obtained using the fixed settings of the TLD readout device. The three curves are normalized separately to unity for ease of comparison. The first and second curves are obtained by directly exposing a TLD to the Ga-67 radionuclide in air with and without attenuation by a 2-cm-thick acrylic plate. The third curve is obtained by placed a TLD into the center of the Ga-67 citrate solution tank (which has a diameter of 15 cm and a height of 30 cm).

obtained using the fixed settings of the TLD readout device. The three curves are normalized separately to unity for easy comparison. The first and second curves are obtained by directly exposing a TLD to the Ga-67 radionuclide in air with and without attenuation by a 2-cm-thick acrylic plate. The third curve is obtained by placing a TLD in the center of the Ga-67 citrate solution tank (diameter, 15 cm; height, 30 cm). Figure 5 shows that the highest peak value of any of the three glow curves is set to unity for easy comparison. After normalizing their peaks, all curves show large variations. The curve for the TLD in the Ga-67 citrate solution shows two almost equal peaks (dotted line in Fig. 5) whereas the others show only one high peak.

The curves reveal the strong effects of the acrylic plate and the water solvent on the second peak of the primary TLD response to the Ga-67 radionuclide ([low–high peaks] solid line in Fig. 5, glow curve of TLD in air). The barely visible second peak in the glow curve of the TLD behind an acrylic plate ([high-low peaks] dot-dashed line in Fig. 5, glow curve of TLD in air behind acrylic plate) indicates that a 2-cm-thick acrylic plate blocks most of the Compton-scattered electrons. In contrast, the directly received gamma rays are also converted into several Compton-scattered electrons, and the transfer of their energy to the TLD molecular structure is clearly reduced as indicated by the temperature response curve ([high–high peaks] dotted line in Fig. 5, glow curve of TLD in water).The Compton-scattered electrons dispersed widely inside the molecular structure of a TLD with more straggling energy compared with those attenuated with only an acrylic plate [23, 31].

Because of the unique plot of the TLD glow curve of the Ga-67 citrate solution, optimization of the TLD readout settings is critical in an actual TLD count. An inappropriate setting may cause an error when recording the TLD glow curve, which can generate an erroneous count–dose calibration curve.

ACKNOWLEDGEMENTS

The authors would like to thank the Buddhist Tzu Chi General Hospital, Taichung Branch for financially supporting this research under Contract No. TTCRD-9911.

REFERENCES

1. Fisher DR. Internal dosimetry for systemic radiation therapy. *Semin Radiat Oncol* 2000;**10**(2):123–32.
2. Yasar D, Tugrul AB. A new approach for the calculation of critical organ dose in nuclear applications. *Appl Radiat Isotopes* 2005;**62**:405–10.
3. Yasar D, Tugrul AB. A comparison of TLD measurements to MIRD estimates of the dose to the tests from Tc-99m in the liver and spleen. *Radiat Meas* 2003;**37**:113–18.
4. Erwin WD, Groch MW, Macey DJ *et al*. A radioimmunoimaging and MIRD dosimetry treatment planning program for radio immunotherapy. *Nucl Med Biol* 1996;**23**(4):525–2.
5. Flynn AA, Green AJ, Boxer GM *et al*. A novel technique, using radioluminography, for the measurement of uniformity of radiolabelled antibody distribution in a colorectal cancer xenograft model. *Int J Radiat Oncol* 1999;**43**(1):183–9.
6. Kim J, Kim J, Kim C *et al*. Calculating specific absorbed fractions with standard Korean male adults. *Radiat Meas* 2010;**45**(1):103–9.
7. Stabin MG, Tagesson M, Thomas SR *et al*. Radiation dosimetry in nuclear medicine *Appl Radiat Isotopes* 1999;**50**(1):73–87.
8. Furhang EE, Sgouros G, Chui CS. Radionuclide photon dose kernels for internal emitter dosimetry. *Med Phys* 1996;**23**:759–64.
9. Stabin MG. Radiopharmaceuticals for nuclear cardiology: radiation dosimetry, uncertainties, and risk. *J Nucl Med* 2008;**49**(9):1555–63.
10. Thomas SR, Gelfand MJ, Burns GS *et al*. Radiation absorbed dose estimates for the liver, spleen and metaphyseal growth complexes in children undergoing Ga-67 citrate scanning. *Radiology* 1983;**146**:817–20.
11. Smith T. Internal exposure of patients and staff in diagnostic nuclear medicine procedures. *L Soc Radiol Prot* 1984;**4**:45–51.
12. Saha GB. *Fundamentals of Nuclear Pharmacy*. New York: Springer-Verlag, 1992.
13. Stabin MG. Health concerns related to radiation exposure of the female nuclear medicine patient. *Environ Health Persp* 1997;**105**(6):1403–9.
14. Shanehsazzadeh S, Jalilian AR, Sadeghi HR *et al*. Determination of human absorbed dose of ^{67}Ga-DTPA-ACTH based on distribution data in rats. *Radiat Prot Dosim* 2009;**134**(2):79–86.
15. UNSCEAR, United Nations Scientific Committee on the Effects of Atomic Radiation. Report of United Nations Scientific Committee on the Effects of Atomic Radiation, Vol. I, INDEX D, 2000.

16. Zuckier LS, Moadel-Sernick RM. *Radiolabeled monoclonal antibodies: Imaging, Nuclear Oncology: Diagnosis and Therapy*. Philadelphia: Lippincott, Williams & Wilkins, 2001, pp. 83–92.
17. ICRP-60. Recommendations of the International Commission on Radiological Protection Technical Report ICRP-60. International Commission on Radiation Protection, 1991.
18. ICRP-26. Recommendations of the International Commission on Radiological Protection Technical Report ICRP-26. International Commission on Radiation Protection, 1977.
19. Arsos G, Moralidis E, Tsechelidis I *et al*. Measurement of glomerular filtration rate with chromium-51 ethylene diamino tetraacetic acid in the presence of gallium-67 citrate: a novel method for the solution of the problem. *Nucl Med Commun* 2011;**32**(3):221–6.
20. Priest ND, Newton D, Day JP *et al*. Human metabolism of aluminium-26 and gallium-67 injected as citrates. *Hum Exp Toxicol* 1995;**14**(3):287–93.
21. Attix FH. *Introduction to Radiological Physics and Radiation Dosimetry*. New York: John Wiley and Sons, 1986.
22. MCNP. *A General Monte Carlo N-Particle Transport Code, V5*, Los Alamos National Laboratory, 2003.
23. Chen CY, Chen HH, Liu KC *et al*. Optimizing the TLD-100 readout system for various radiotherapy beam doses using the Taguchi methodology. *Appl Radiat Isotopes* 2010;**68**(3):481–8.
24. ICRU-48. Phantoms and computational models in therapy, diagnosis and protection ICRU-48. Bethesda: International Commission on Radiation Units and Measurement, 1992.
25. Tanner JE, Piper RK, Leonowich JA *et al*. Verification of an effective dose equivalent model for neutron. *Radiat Prot Dosim* 1992;**44**:171–4.
26. MIRDOSE 3. Radiation Internal Dose Information Center (RIDIC), Oak Ridge Institute For Science and Education (ORISE), 1987.
27. Shanehsazzadeh S, Lahooti A, Sadeghi HR *et al*. Estimation of human effective absorbed dose of ^{67}Ga-cDTPA-gonadorelin based on biodistribution rat data. *Nucl Med Commun* 2011;**32**(1):37–43.
28. MIRD Dose Estimate Report No. 2. Radiation absorbed dose for Ga-66, Ga-67, Ga-68 and Ga-72 citrate. *J Nucl Med* 1973;**14**:755–6.
29. Society of Nuclear Medicine. *Society of Nuclear Medicine Procedure Guideline for Gallium Scintigraphy in Inflammation Version 3.0*, approved June 2, 2004. http://interactive.snm.org/docs/Gallium_Scintigraphy_in_Inflammation_v3.pdf.
30. Turner JE. *Atoms, Radiation and Radiation Protection, 3rd Edition*. New York: John Wiley & Sons, Inc., 2007.
31. Chu TC, Lin SY, Hsu CC *et al*. The response of a thermoluminescent dosimeter to low energy protons in the range 30–100keV. *Appl Radiat Isotopes* 2001;**55**(5):679–84.